GLOBAL ELASTIC SHEAR BUCKLING ANALYSIS OF CORRUGATED PLATES WITH EDGES ELASTICALLY RESTRAINED AGAINST ROTATION

Chawalit MACHIMDAMRONG*, Eiichi WATANABE** and Tomoaki UTSUNOMIYA***

*Student member of JSCE, Graduate Student, Dept. of Civil Eng., Kyoto University
Yoshida-honmachi, Sakyo-ku, Kyoto 606-8501, Japan
**Fellow of JSCE, Ph. D., Dr. Eng., Professor, Dept. of Civil Eng., Kyoto University
Yoshida-honmachi, Sakyo-ku, Kyoto 606-8501, Japan
***Member of JSCE, Dr. Eng., Associate Professor, Dept. of Civil Eng., Kyoto University
Yoshida-honmachi, Sakyo-ku, Kyoto 606-8501, Japan

This paper presents an estimation of global elastic shear buckling strength of corrugated plates considering the influence of elastically rotational restraint on boundary edges. The corrugated plate possesses higher shear buckling strength comparing to a flat one and it has been used to replace concrete web in PC box girder in recent bridge construction in Japan. In this study, the corrugated plate is considered as an orthotropic flat plate. Thick rectangular plate theory is used and Rayleigh-Ritz method is utilized in extracting eigenvalues. Elastically rotational restraint on boundary edges is taken into account in the form of rotational spring in the analysis. Prediction of buckling strengths of corrugated plates is carried out using the Rayleigh-Ritz method, which was proved to be consistent with those as predicted by a proposed formula using a design manual and was found also to cover the more general cases of elastically rotational restraint on the boundary edges showing transition curve of plate buckling strengths from the case of simple support to the case of clamped support. A finite element analysis was also carried out to verify the accuracy of the proposed method. As a result, a discrepancy is found between the buckling strength by the finite element analysis and that by the proposed analysis; however, the formula adopted in the design manual may be thought to be conveniently used because it can lead to the conservative design.

Key Words: Global elastic shear buckling strength, Corrugated web plates, Elastically rotational restraint, Rayleigh-Ritz method, Mindlin plate theory.

1. Introduction

Corrugated steel plates have been recently utilized in construction of new bridges in Japan. Concrete webs in conventional PC box girder are replaced with corrugated steel webs. Corrugated shape of the plate acts as vertical stiffeners and consequently increases shear buckling strength of the girder. This helps reducing the weight of the structure. However, in the estimation of global elastic shear buckling strength of the plate, estimation formula for the design was derived basing on thin plate theory and a support condition was considered as simple support [1]. This formula is used and noted in Design Manual of PC box Girders with Corrugated Steel Web proposed by Research Group of Composite Structure with Corrugated Steel Web [2].

The aim of this study is to make a more precise prediction of global elastic shear buckling strength of the plates. Especially, elastically rotational restraint on the boundary edges is considered and its influence on plate's buckling strength is investigated. Since sometimes, unfirm or partial attachment at the support of the plate unintentionally causes decrement of shear buckling strength and it is a question of how serious it affects.

The estimation is based on equivalent orthotropic plate consideration. Thick rectangular plate theory or Mindlin plate theory is used. On the boundary edges, elastically rotational restraint is taken into account in form of elastically rotational spring.

Rayleigh-Ritz method is employed, and the relevant energy functions are obtained. Trigonometric series are selected as trial functions, in which they meet the requirements on the boundary condition. Global elastic shear buckling strength of the plate is calculated by standard eigenvalue extraction procedure. Elastic constant estimation method that is used to transform a corrugated plate to an equivalent orthotropic flat plate is presented.

Estimation of buckling strengths of six simple corrugated plates, different in degrees of inclination and plate's dimensions is carried out. By varying stiffness of rotational spring on the boundary edges, its influence on buckling strength is examined. The plates are also modeled and analyzed in finite element analysis, in which buckling strengths are calculated.

Conclusion is made on the influence of rotational restraint on the boundary edges to buckling strengths of the plates and discrepancy between finite element analysis and this analysis.

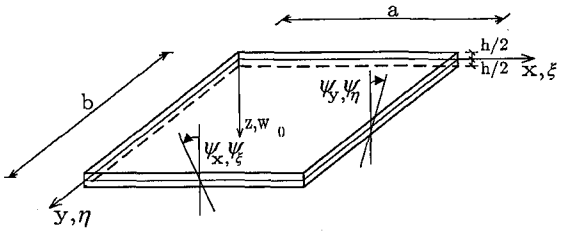

Figure 1: Mindlin plate geometry

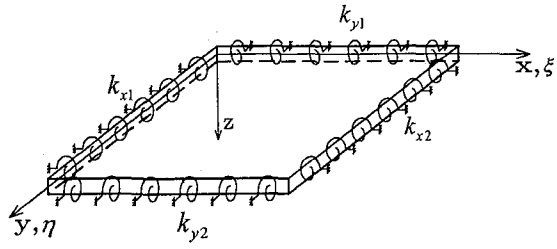

Figure 2: Plate with rotational springs

2. Orthotropic Rectangular Mindlin Plate

Theoretical analysis is based on the assumption that a corrugated web can be analyzed as a rectangular orthotropic flat plate with uniform thickness. This assumption on an orthotropic flat plate simplification was given by Easley et al. [1] as (1) the number of repeating corrugation sections in a diaphragm is usually large and their dimensions small, compared to the overall dimensions of the diaphragm; (2) the interest is in overall buckling behavior and not in localized effects; and (3) the buckle patterns which appear in test specimens seem to be independent of local corrugation shapes [1].

The displacement fields of Mindlin plate theory [3], can be expressed as follows:

$$\begin{aligned} u(x,y,z) &= z\psi_x(x,y), \\ v(x,y,z) &= z\psi_y(x,y), \\ w(x,y,z) &= w_0(x,y), \end{aligned} \tag{1}$$

where w_0 is displacement along z-axis in the middle surface, ψ_x and ψ_y are cross-sectional rotations in x and y-direction, respectively (Figure 1).

By infinitesimal displacement theory, the cross-sectional rotations of plate (ψ), shear deformations (γ) and displacement of the plate are related as follow:

$$\begin{aligned} \psi_x &= \gamma_{xz} - \frac{\partial w_0}{\partial x}, \\ \psi_y &= \gamma_{yz} - \frac{\partial w_0}{\partial y}. \end{aligned} \tag{2}$$

The relation between stress and strain for orthotropic material in plane stress condition is:

$$\sigma = D\epsilon, \tag{3}$$

where, σ, ε, and D in matrix form are:

$$\sigma^T = [\ \sigma_x \quad \sigma_y \quad \tau_{xy} \quad \tau_{xz} \quad \tau_{yz}\ ], \tag{4}$$

$$\epsilon^T = [\ \varepsilon_x \quad \varepsilon_y \quad \gamma_{xy} \quad \gamma_{xz} \quad \gamma_{yz}\ ], \tag{5}$$

$$D = \begin{bmatrix} \frac{E_x}{(1-\nu_x\nu_y)} & \frac{\nu_x E_y}{(1-\nu_x\nu_y)} & 0 & 0 & 0 \\ \frac{\nu_y E_x}{(1-\nu_x\nu_y)} & \frac{E_y}{(1-\nu_x\nu_y)} & 0 & 0 & 0 \\ 0 & 0 & G_{xy} & 0 & 0 \\ 0 & 0 & 0 & K_x G_{xz} & 0 \\ 0 & 0 & 0 & 0 & K_y G_{yz} \end{bmatrix}. \tag{6}$$

Here, E_x and E_y are modulus of elasticity in x- and y-directions, respectively. ν_x characterizes the transverse strain in y-direction, when the material is stressed in x-direction, and ν_y characterizes the transverse strain in x-direction, when the material is stressed in x-direction. K_x and K_y are transverse shear correction coefficients in x-z and y-z planes. Shear modulus of elasticity in x-y, x-z and y-z planes are G_{xy}, G_{xz} and G_{yz}, respectively.

Strain energy, U_1, stored in plate can be obtained from the above strain-displacement relation and Hook's law as below:

$$\begin{aligned} U_1 &= \int_V \epsilon^T D\epsilon \, \mathrm{d}V \\ &= \frac{1}{2}\int_0^b\int_0^a \left\{ \left[(\nu_y D_x + \nu_x D_y)\left(\frac{\partial\psi_x}{\partial x}\frac{\partial\psi_y}{\partial y}\right) \right.\right. \\ &\quad + D_x\left(\frac{\partial\psi_x}{\partial x}\right)^2 + D_y\left(\frac{\partial\psi_y}{\partial y}\right)^2 + D_{xy}\left(\frac{\partial\psi_x}{\partial y} + \frac{\partial\psi_y}{\partial x}\right)^2 \Big] \\ &\quad + K_x h G_{xz}\left(\psi_x + \frac{\partial w_0}{\partial x}\right)^2 \\ &\quad \left. + K_y h G_{yz}\left(\psi_y + \frac{\partial w_0}{\partial y}\right)^2 \right\} \mathrm{d}x\,\mathrm{d}y, \end{aligned} \tag{7}$$

where h denotes plate thickness, and $D_x = \frac{E_x h^3}{12(1-\nu_x\nu_y)}$, $D_y = \frac{E_y h^3}{12(1-\nu_x\nu_y)}$, $D_{xy} = G_{xy}\frac{h^3}{12}$.

Edge elastically restrained against rotation as shown in Figure 2 is considered due to the fact that actual boundary condition of a real system is mostly not classical, but somewhere between simple support and fixed support [4]. Rotational spring constants in x-direction at $x = 0$ and $x = a$, in y-direction at $y = 0$ and $y = b$ are designated as k_{x1}, k_{x2}, k_{y1}, and k_{y2}, respectively. Strain energy stored in rotational springs, U_2, is:

$$\begin{aligned} U_2 &= \frac{1}{2}\int_0^a \left(k_{y1}\psi_y^2|_{y=0} + k_{y2}\psi_y^2|_{y=b}\right) \mathrm{d}x \\ &\quad + \frac{1}{2}\int_0^b \left(k_{x1}\psi_x^2|_{x=0} + k_{x2}\psi_x^2|_{x=a}\right) \mathrm{d}y. \end{aligned} \tag{8}$$

Potential energy of the plate , V_1, which is of in-plane shear load, N_{xy}, as in Figure 3 is:

$$V_1 = -\int_0^b\int_0^a N_{xy}\left(\frac{\partial w_0}{\partial x}\frac{\partial w_0}{\partial y}\right) \mathrm{d}x\,\mathrm{d}y. \tag{9}$$

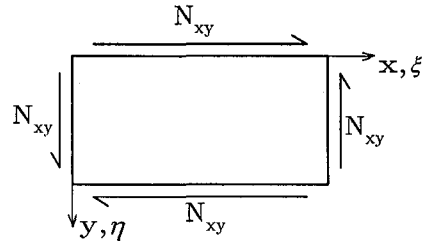

Figure 3: Plate under in-plane shear

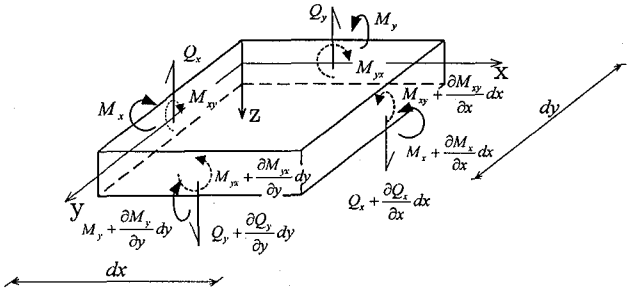

Figure 4: Force notations of plate

Potential energy of external loadings, V_2, as shown in Figure 4 is:

$$V_2 = \int_0^a \Big[\left(M_y\psi_y + M_{yx}\psi_x + Q_y w_0\right)|_{y=b} - \left(M_y\psi_y + M_{yx}\psi_x + Q_y w_0\right)|_{y=0} \Big] \mathrm{d}x + \int_0^b \Big[\left(M_x\psi_x - M_{xy}\psi_y + Q_x w_0\right)|_{x=a} - \left(M_x\psi_x - M_{xy}\psi_y + Q_x w_0\right)|_{x=0} \Big] \mathrm{d}y. \quad (10)$$

Here M_x is bending moment in x-direction, M_{xy} is twisting moment in x-direction (around x-axis along y-direction edges), and so on.

The total potential energy function of rectangular orthotropic Mindlin plate can then be written as follows:

$$\Pi = U_1 + U_2 - V_1 - V_2. \quad (11)$$

3. Rayleigh-Ritz Method

In calculation of plate's buckling strength, Rayleigh-Ritz method is used in this study. Essential to this method is selection of trial function, where trigonometric series are used.

The trigonometric series satisfying hard type simply supported boundary edge condition [5] are shown below:

$$w_0(\xi,\eta) = \sum_{i=1}^{m}\sum_{j=1}^{n} A_{ij}\sin(i\pi\xi)\sin(j\pi\eta),$$
$$\psi_\xi(\xi,\eta) = \sum_{i=1}^{p}\sum_{j=1}^{q} B_{ij}\cos(i\pi\xi)\sin(j\pi\eta),$$
$$\psi_\eta(\xi,\eta) = \sum_{i=1}^{r}\sum_{j=1}^{s} C_{ij}\sin(i\pi\xi)\cos(j\pi\eta). \quad (12)$$

Here dimensionless variables, ξ and η are employed, by replacing $\xi = x/a$ and $\eta = y/b$. These trigonometric series yield zero displacement along all edges, zero x-direction rotation (ψ_ξ) on $y = 0$ and $y = b$ edges, but arbitrary on $x = 0$ and $x = a$ edges, and in the same fashion for y-direction rotation (ψ_η). The total potential energy equation, Π is obtained by substituting Equation 7, 8, 9 and 10 into Equation 11. It is then made dimensionless and set $\alpha = a/b$. It is shown below:

$$\Pi = \frac{1}{2\alpha}\int_0^1\int_0^1 \Bigg\{ \Big[\alpha\left(\nu_y D_x + \nu_x D_y\right)\left(\frac{\partial\psi_\xi}{\partial\xi}\frac{\partial\psi_\eta}{\partial\eta}\right) + D_x\left(\frac{\partial\psi_\xi}{\partial\xi}\right)^2 + \alpha^2 D_y\left(\frac{\partial\psi_\eta}{\partial\eta}\right)^2 + D_{xy}\left(\alpha\frac{\partial\psi_\xi}{\partial\eta} + \frac{\partial\psi_\eta}{\partial\xi}\right)^2\Big] + K_x h G_{xz}\left(a\psi_\xi + \frac{\partial w_0}{\partial\xi}\right)^2 + \alpha^2 K_y h G_{yz}\left(b\psi_\eta + \frac{\partial w_0}{\partial\eta}\right)^2 + 2\alpha N_{xy}\left(\frac{\partial w_0}{\partial\xi}\frac{\partial w_0}{\partial\eta}\right) \Bigg\} \mathrm{d}\xi\,\mathrm{d}\eta + \frac{\alpha D_y}{2}\int_0^1 \left(K_{y1}\psi_\eta^2|_{\eta=0} + K_{y2}\psi_\eta^2|_{\eta=1}\right)\mathrm{d}\xi + \frac{D_x}{2\alpha}\int_0^1 \left(K_{x1}\psi_\xi^2|_{\xi=0} + K_{x2}\psi_\xi^2|_{\xi=1}\right)\mathrm{d}\eta. \quad (13)$$

Note that, potential energy of loading expressed by Equation 10 vanishes naturally for the case of hard type simple support edge. Substituting trigonometric series, Equation 12, into dimensionless total potential energy equation, Equation 13 and then differentiate the function with respect to unknowns, A_{ij}, B_{ij}, and C_{ij}, one obtains:

$$\frac{\partial\Pi}{\partial A_{ij}} = \frac{h}{4\alpha}\Big\{K_x G_{xz}(i\pi)^2 + \alpha^2 K_y G_{yz}(j\pi)^2\Big\}A_{ij} + \frac{aK_x h G_{xz}}{4\alpha}(i\pi)B_{ij} + \frac{\alpha b K_y h G_{yz}}{4}(j\pi)C_{ij} + N_{xy}\sum_{\substack{k=1\\ i\pm k=\text{odd}}}^{m}\sum_{\substack{l=1\\ j\pm l=\text{odd}}}^{n}\frac{8ijkl}{(k^2-i^2)(j^2-l^2)}A_{kl} = 0, \quad (14)$$

$$\frac{\partial\Pi}{\partial B_{ij}} = \frac{aK_x h G_{xz}}{4\alpha}(i\pi)A_{ij} + \frac{1}{4\alpha}\Big\{D_x(i\pi)^2 + \alpha^2 Dxy(j\pi)^2 + K_x h G_{xz}a^2\Big\}B_{ij} + \frac{D_x}{2}\sum_{k=1}^{p}\Big\{k_{x1} + k_{x2}(-1)^{i+k}\Big\}B_{kj} + \frac{1}{8}\Big\{(\nu_x D_y + \nu_y D_x) + 2D_{xy}\Big\}(i\pi)(j\pi)C_{ij} = 0, \quad (15)$$

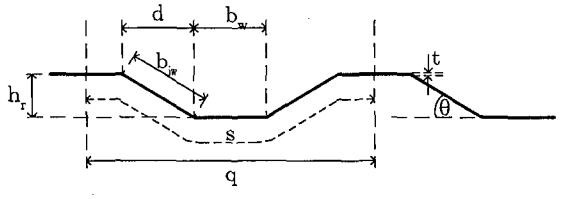

Figure 5: Cross section geometry of corrugated web

$$\frac{\partial \Pi}{\partial C_{ij}} = \frac{\alpha b K_y h G_{yz}}{4}(j\pi)A_{ij} + \frac{1}{8}\Big\{(\nu_x D_y + \nu_y D_x) + 2D_{xy}\Big\}(i\pi)(j\pi)B_{ij} + \frac{1}{4\alpha}\Big\{\alpha^2 D_y (j\pi)^2 + D_{xy}(i\pi)^2 + \alpha^2 K_y h G_{yz} b^2\Big\}C_{ij} + \frac{\alpha^2 D_y}{2}\sum_{l=1}^{s}\Big\{k_{y1} + k_{y2}(-1)^{j+l}\Big\}C_{il} = 0. \quad (16)$$

The above equations can be rearranged and written in matrix form, to solve for unknown coefficients as follows:

$$\begin{bmatrix} K'_{11} & K'_{12} & K'_{13} \\ \vdots & K'_{22} & K'_{23} \\ \text{symm} & \cdots & K'_{33} \end{bmatrix} \begin{pmatrix} A_{ij} \\ B_{ij} \\ C_{ij} \end{pmatrix} - N_{xy} \begin{pmatrix} A_{ij} \\ 0 \\ 0 \end{pmatrix} = 0. \quad (17)$$

If the number of terms in Equation 12, m, n, p, q, r and s are selected equally, size of stiffness matrix will be $3n^2$ by $3n^2$. Global elastic shear buckling strength of a plate is then calculated by finding the solution of eigenvalue Equation 17. This can be done by usual eigenvalue extraction procedure. In the next section, for convenience, we define dimensionless parameters of elastically rotational springs in x- and y-directions by:

$$K_{x1} = \frac{a k_{x1}}{D_x}, \quad \text{and} \quad K_{x2} = \frac{a k_{x2}}{D_x},$$
$$K_{y1} = \frac{b k_{y1}}{D_y}, \quad \text{and} \quad K_{y2} = \frac{b k_{y2}}{D_y}. \quad (18)$$

4. Elastic constants estimation

In order to carry out an analysis developed in previous section, a corrugated plate must be transformed into an equivalent homogeneous orthotropic thick plate with appropriate structural properties. Elastic constants required (see Equation 13) for this purpose are flexural stiffness in two principal directions (D_x, D_y), twisting stiffness (D_{xy}), plate stiffness ($\nu_x D_y + \nu_y D_x$) and transverse shear stiffness in two principal directions ($K_x h G_{xz}$, $K_y h G_{yz}$). Definitions of dimensions of corrugated plate are illustrated in Figure 5.

From here on, the direction of plate's lower flexural stiffness is referred as x-direction and the direction of plate's higher flexural stiffness as y-direction (which corresponds with that shown in Figure 6).

4.1. Flexural stiffness

Equivalent flexural stiffness in x-direction, D_x, and in y-direction, D_y, can be approximated by [1] [6]:

$$D_x = \frac{q}{s}\frac{Et^3}{12}, \quad (19)$$
$$D_y = \frac{EI_y}{q}. \quad (20)$$

Moment of inertia in y-direction, I_y in Equation 20, can be calculated by the following equation:

$$I_y = 2(b_w t\frac{h_r^2}{4} + \frac{b_w t^3}{12} + \frac{b_{iw}^3 t}{12}\sin^2\theta). \quad (21)$$

Plate stiffness $(\nu_x D_y + \nu_y D_x + 2D_{xy})/2$ in the analysis is usually neglected [6]. However, in this study, only the term involving D_{xy} was retained in the same manner with Easley et al. [1]. The terms $(\nu_x D_y + \nu_y D_x)$ can also be neglected when $D_y \gg D_x$, which is usually true for corrugated plate [1].

In the code proposed by Research Group of Composite Structure with Corrugated Steel Web [2] on the section of global shear buckling strength, the equivalent flexural stiffness are noted as below:

$$D_x = \frac{Et^3}{12(1-\nu^2)}, \quad (22)$$
$$D_y = \frac{s}{q}\frac{E(t^3 + th_r^2)}{6}. \quad (23)$$

Equation 19 estimates flexural stiffness of the plate in the same way as a curved beam, while Equation 22 assumes the plate as a flat plate with no corrugation. Flexural stiffness in y-direction is exactly estimated in Equation 20 and approximately in Equation 23.

4.2. Twisting stiffness

Effective shear modulus of elasticity, G_{xy}^{eff} in the equation must be considered regarding corrugate configuration and attachment method.

For a corrugated plate attaches continuously to the supports, deformation due to uniform in-plane shear load is of uniform shear strain throughout the material [7] [8]. In short, the shear modulus, G, of material is equal to the ratio of uniform shear stress, F/bt, and shear strain in the corrugated plate is u_0/s (Figure 6). Here, s is a developed width of one corrugation, equals to $2b_w + 2b_{iw}$. However, for equivalent orthotropic plate, the shear strain in the plate, u_0/q. Thus, effective shear modulus, G_{xy}^{eff} can be defined as $G_{xy}^{\text{eff}} = Gq/s$. The equivalent twisting stiffness, D_{xy} of corrugated plate, after substituting the relation $G = E/2(1+\nu)$ of isotropic material, can be expressed as below:

$$D_{xy} = \frac{s}{q}\frac{Et^3}{6(1+\nu)}, \quad (24)$$

which is exactly the same as used by Easley et al. [1].

In the case of discrete attachment, the effective shear modulus is lower than that given in Equation 24, depending on the method of attachment (see [7], [8] for examples).

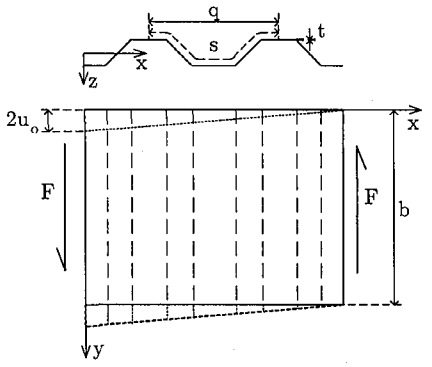

Figure 6: Corrugated plate under simple in–plane shear force

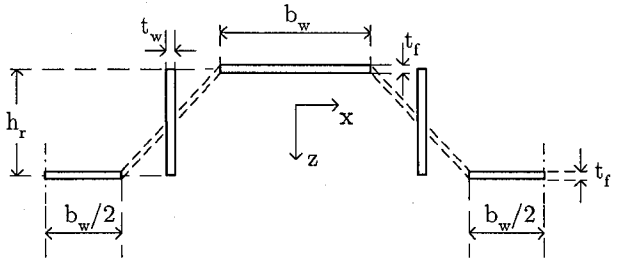

Figure 7: Transformed section of corrugated web for transverse shear stiffness approximation

4.3. Transverse shear stiffness

In order to estimate the transverse shear stiffness in y-direction, $K_y h G_{yz}$, one wavelength of corrugated web is simply considered as a simple beam. Inclined strips of cross section of corrugated web were made presumably right angle to the remaining parts with the equivalent cross section area, as shown in Figure 7. The formula for estimating transverse shear correction factor for thin-walled rectangular tube, which is mathematically equivalent to the transformed section, is as below [9]:

$$K_y = \frac{H_1}{H_2 + r\nu(H_3 + H_4 + H_5 + H_6)}, \qquad (25)$$

where

$$H_1 = 10(1+3m)^2,$$
$$H_2 = 12 + 72\ m + 150m^2 + 90m^3 + 30n^2\ m(1+m),$$
$$H_3 = -2 + 3m + 15m^2,$$
$$H_4 = -n^2(25m + 15m^2),$$
$$H_5 = -n^2(15m + 45m^2),$$
$$H_6 = -15m - 45m^2,$$
$$m = \frac{b_w}{h_r}\frac{t_f}{t_w}, \quad n = \frac{b_w}{h_r}, \quad r = \frac{G}{E}$$
$$t_f = t, \quad t_w = \frac{b_{iw} t}{h_r}.$$

The thickness, h, in $K_y h G_{yz}$ for this transverse shear stiffness is replaced with the average thickness of corrugated section:

$$t_{av} = \frac{s}{q} t. \qquad (26)$$

Shear modulus, G_{yz} is simply shear modulus of the plate, G. For the transverse shear stiffness factor in x-direction, $K_x h G_{xz}$, the average thickness of corrugated section is used and shear correction factor, K_x, is taken equal to $5/(6-\nu)$ [10].

5. Calculation

Three different simple geometric shapes of corrugated plate are studied. The wavelength of each corrugated shape (q) is fixed at 125 mm. Equal panel width ($b_w = b_{iw}$) is considered. Only the degree of panel inclination (θ) is varied as 30, 37 and 45 degrees. The thickness of the plates is taken equally to 2 mm constantly. The relevant dimension parameters, as shown in Figure 5 are then derived based upon above criteria. Material is assumed elastic with Young modulus of 2.06×10^{11} N/m^2, and Poisson's ratio of 0.30.

Calculations are made on 6 plates, comprise of all three degrees of panel inclination with plate dimensions ($a \times b$) of 1 m $\times$ 1 m and 2 m $\times$ 1 m. In each case, only simple or fixed support edges in the x-direction are considered. On the other hand, supported edges in y-direction are considered to be restrained by elastically rotational spring and their stiffness are varied equally from 1.0 Nm/m to 10^{10} Nm/m to cover possible stiffness of simple support to fixed support.

5.1. Rayleigh-Ritz analysis

Elastic constants necessary in Rayleigh-Ritz analysis are estimated as described in previous section. Flexural stiffness, D_x and D_y estimated by Equations 19 and 20 are denoted as elastic estimation formulas 1, and of Equations 22 and 23 as elastic estimation formulas 2. In every case, both two elastic estimation formulas are utilized in Rayleigh-Ritz analysis. The dimension parameters and calculated elastic constants of the plates are summarized in Table 1.

The number of terms in trigonometric series employed in calculation are 256 terms (16×16) in each variable. This number is so selected to avoid computational error and not to overload the computer. It is found that a calculation with maximum capacity of 400 terms (20×20) reveals a difference in results within 1% compared to that calculated with 256 terms but need computational time more than 4 times longer.

5.2. Finite element analysis

Finite element method is also used to compute the buckling strengths of the plates. Figure 8 shows a typical model used in the finite element analysis. Element used to model corrugated plate is 9-nodes shell element, S9R5 available in ABAQUS, a finite element analysis program. Four shell elements are used along panel width, but 50 elements in perpendicular direction. Every nodes on the plate boundary are rotationally restrained with respect to center line of the corrugation to represent rotation of middle plane of the

Table 1: Parameters of corrugated plates in this study

Plate's parameters	degree of inclination		
	30	37	45
$q\ (mm)$	125		
$s\ (mm)$	133.97	138.99	146.45
$h_r\ (mm)$	16.75	20.91	25.89
$D_x\ (10^2 Nm^2/m)^a$	1.2814	1.2351	1.1723
$D_y\ (10^4 Nm^2/m)^a$	2.0715	3.3469	5.4000
$D_x\ (10^2 Nm^2/m)^b$	1.5092	1.5092	1.5092
$D_y\ (10^4 Nm^2/m)^b$	2.0936	3.3698	5.4241
$D_{xy}\ (10^3 Nm^2/m)$	2.2646	3.0543	3.2181
K_x	0.8772	0.8772	0.8772
K_y	0.2644	0.3098	0.3463

[a]elastic estimation formulas 1 (Equations 19 & 20)
[b]elastic estimation formulas 2 (Equations 22 & 23)

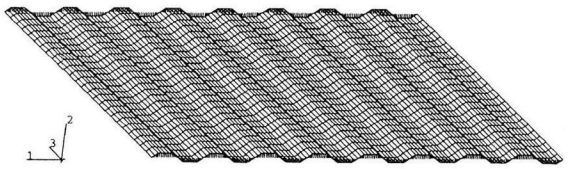

Figure 8: Finite element model of 1 m × 1 m plate

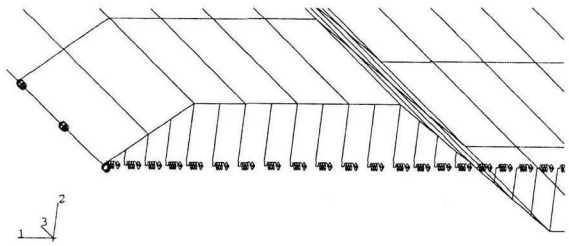

Figure 9: Spring arrangement on finite element model

plate. This is achieved by connecting rigid beam elements, RB3D2 from the nodes to ideal nodes on the center line as shown in Figure 9. Then, spring element of type SPRING1 is used to restrain the ideal nodes to ground. Also, all of the ideal nodes on each edge are constrained to move in the center line connecting their corresponding corner nodes.

5.3. Calculation results

The results of the calculation are shown in Figure 10 to Figure 15. Note here that, $k_x = 0$ and $k_x = \infty$ in the figures denote to simple and fixed support edges in x-direction, respectively.

Two horizontal lines in the figures denote estimated buckling strengths calculated by the estimation formula noted in Design Manual [2]. Upper and lower lines represent estimated buckling strengths of the plates with fixed and simple support edges in y-direction, respectively. This estimation formula is shown as follows:

$$P^e_{cr,G} = 36\beta \frac{\sqrt[4]{D_x D_y^3}}{b}, \qquad (27)$$

where β is set to either 1.0 or 1.9 for plate with simple

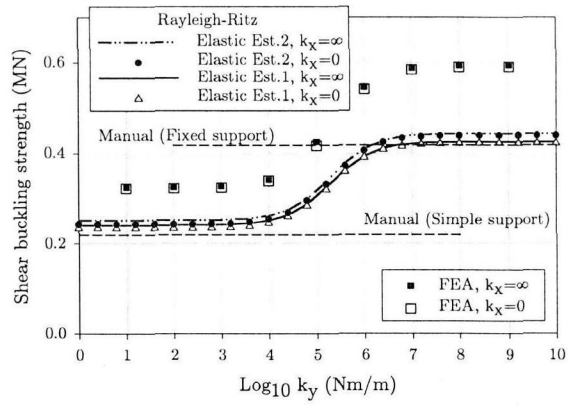

Figure 10: Shear buckling strength of $\theta = 30°$, 1 m × 1 m plate

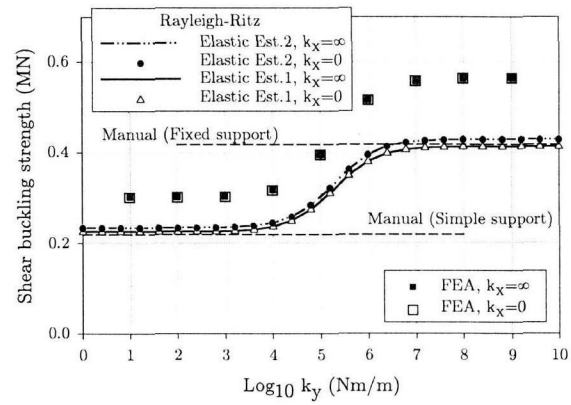

Figure 11: Shear buckling strength of $\theta = 30°$, 2 m × 1 m plate

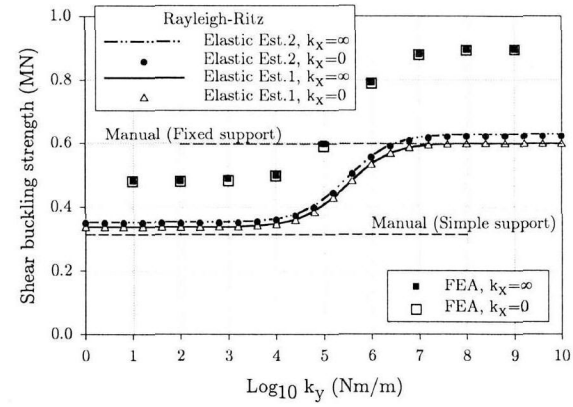

Figure 12: Shear buckling strength of $\theta = 37°$, 1 m × 1 m plate

or fixed support edges in y-direction, respectively. Flexural stiffness formulas according to Equation 22 and 23 (elastic estimation formulas 2) are used in the equation.

It is clear that this Rayleigh-Ritz analysis yield buckling strengths in agreement with those calculated by Equation 27, both for simple and fixed support edges. However, they underestimate buckling strength com-

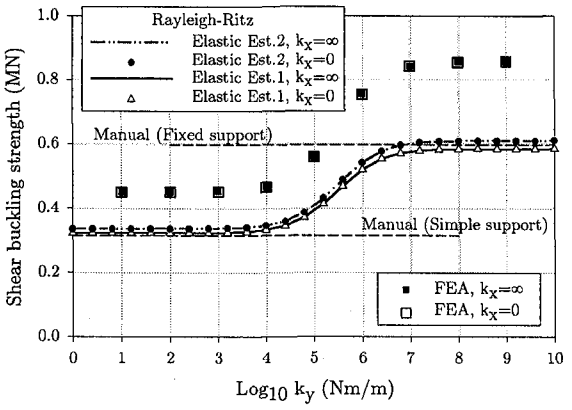

Figure 13: Shear buckling strength of $\theta = 37°$, 2 m × 1 m plate

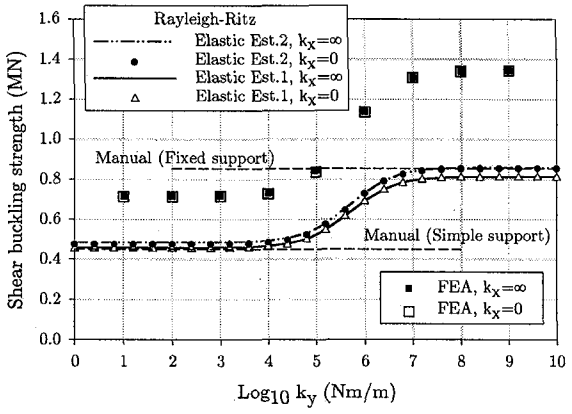

Figure 14: Shear buckling strength of $\theta = 45°$, 1 m × 1 m plate

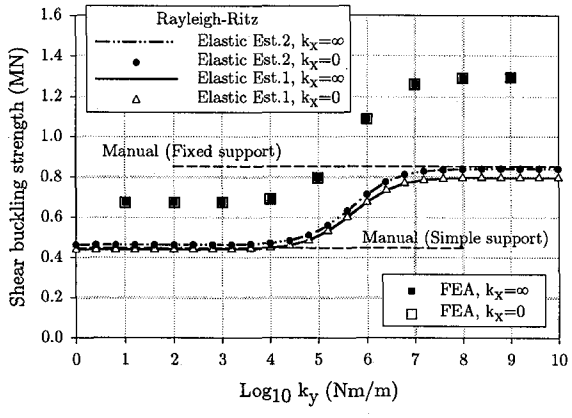

Figure 15: Shear buckling strength of $\theta = 45°$, 2 m × 1 m plate

paring to result of finite element analysis.

From the figures, buckling strengths estimated by finite element analysis are higher than buckling strength predicted by Rayleigh-Ritz analysis for the equivalent orthotropic plate. The difference in buckling strength increases as a parameter θ increases (so reduces degree of the angle measuring between adjacent panels). It is thought that deformation in each panel of corrugated plate is somewhat constrained by adjacent panels and this helps stiffening the panels to some extent.

Then, it requires a modification to the estimation method, for example in Equation 27, to compensate for this difference. The equation can be simply modified as below:

$$P^{e}_{cr,G} = 36\beta k_c \frac{\sqrt[4]{D_x D_y^3}}{b} \tag{28}$$

where k_c is a correcting function for buckling strength which takes into account of other parameters of corrugated geometry including angle of inclination of the corrugation, θ.

For plates with high aspect ratio (i.e. 2 m × 1 m), both finite element analysis and Rayleigh-Ritz analysis yield buckling strengths lower than plates with low aspect ratio (i.e. 1m × 1 m). This is exact with what was expected from elementary shear buckling analysis of plate.

5.4. Effect of rotational restrain

Regardless of this difference in buckling strengths, similarity of graph shapes between this Rayleigh-Ritz analysis results and finite element analysis results is found in every figure. That means the contribution of rotational restraint on the edges to buckling strength of the corrugated plates can be solely explained by this Rayleigh-Ritz analysis.

As can be seen in the figures, increasing of stiffness of rotational restrain on the edges in y-direction obviously shifts buckling strength of the plates from those of simple support edge to fixed support edge. On the other hand, for a given rotational restraint stiffness in y-direction, no significant difference in buckling strength is found between simple and fixed support edges in x-direction. It is concluded here that support edges in the direction of plate's lower flexural stiffness (x-direction) can be neglected in estimation of buckling strength of corrugated plates.

Regarding to the elastic estimation formulas exploited in this Rayleigh-Ritz analysis, both yield buckling strengths close to each other, and they clearly reveal the shifting of buckling strength. However, elastic estimating formulas 2 yield buckling strengths higher than formulas 1.

When rotational spring constant in y-direction is made dimensionless by Equation 18, it is found that there is a specific transition zone of buckling strength from that of simple support edge to fixed support edge. The relation can be seen in Figure 16 in which each shear buckling strength plot derived by finite element method is comparatively normalized to a range of zero to one. The x-axis of each plot is made dimensionless, however by elastic estimation formula 2. It is clear that the transition zone spans over only a specific range for every plate, regardless of corrugated shapes, and dimensions. The dimensionless rotational spring constant of about 10^{-2} is found as a lower bound or simply support

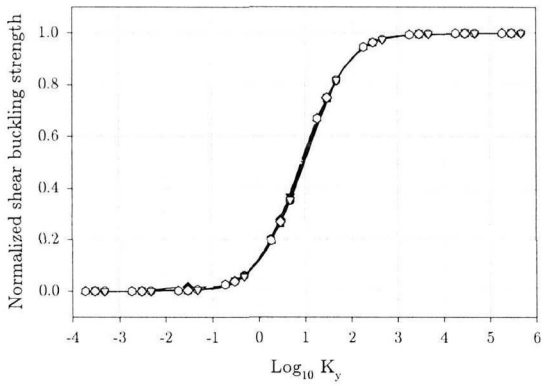

Figure 16: Normalized buckling strength plots (only finite element analysis results)

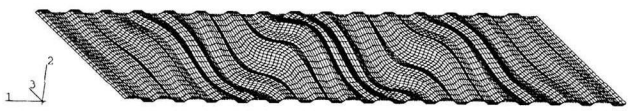

Figure 17: Buckling shape of 2 m × 1 m plate

bound. For upper bound or fixed support bound, the dimensionless value is about 10^4.

Figure 17 shows a typical buckling shape of a 2 m × 1 m plate obtained from finite element analysis.

6. Conclusion

This Rayleigh-Ritz analysis reveals the influence of rotational restraint on global elastic buckling strength of corrugated plates. The formula for the estimation of the global elastic shear buckling strength adpted in design manual yields values consistent to the results of this Rayleigh-Ritz analysis. However, this study is extended to cover the boundary condition not only simply or fixed supported, but elastically rotational restrained.

Influence of elastically rotational restraint is investigated and it is found that type of support edge in the direction of plate's lower flexural stiffness, either simple or fixed support has little effect on buckling strength. On the other hand, buckling strength depends greatly on the magnitude of rotational restraint in the direction of plate's higher flexural stiffness. Also found is that there is a specific range of dimensionless rotational spring constant in the direction of plate's higher flexural stiffness that causes buckling strength to vary from that of simple support to fixed support. This range is approximately about 10^{-2} to 10^4. It is independent of corrugated shape or dimensions of the plate. If this rotational restraint can be measured, it can be used to ensure the strength of the corrugated plates whether do they meet with criteria at the design time or not

Nevertheless, both the Rayleigh-Ritz analysis and estimation formula noted in design manual yield buckling strengths lower than those obtained from finite element analysis. One way of improving the prediction was suggested in the text by utilizing a correcting function that takes into account the corrugated geometry of the plates such as the variation of the neutral plane of the plates. Another is to consider the actual corrugated geometry in the analysis, which is mathematically very difficult and it requires further extensive researches on this subject.

Although, the accurate estimation on global elastic shear buckling strength of corrugated plate is still required, this Rayleigh-Ritz and the estimating formula noted in design manual give a buckling strength in a conservative side and it may be safe to use in design.

There remain many points requiring further research in area of analysis of shear buckling strength of corrugated plate. One is to extend the scope of buckling analysis to include elastoplastic buckling. Another point expected to be carried out in the future is to perform experiments to check with the analysis which help confirming theoretical analysis and in developing correcting function. Also, further study is needed on how to evaluate rotational stiffness of boundary edge.

References

[1] Easley, J. T., and McFarland, D. E. (1969), "Buckling of Light-Gage Corrugated Metal Shear Diaphragms." J. Struct. Div., ASCE, 95(ST7), 1497–1516.

[2] Research Group of Composite Structure with Corrugated Steel Web (1998), Design manual of PC box girders with corrugated steel webs (Draft). (in Japanese)

[3] Mindlin, R. D. (1951), "Influence of Rotatory Inertia and Shear on Flexural Motions of Isotropic, Elastic Plates." J. Appl. Mech., 18(March), 1031–1036.

[4] Chung, J. H., Chung, T. Y., and Kim, K. C. (1993), "Vibration Analysis of Orthotropic Mindlin Plates with Edges Elastically Restrained Against Rotation." J. Sound Vib., 163(1), 151–163.

[5] Liew, K. M., Wang, C. M., Xiang, Y., and Kitipornchai, S. (1998), Vibration of mindlin plates: programming the p-version ritz method, Elsevier, Netherlands.

[6] Peterson, J. M., and Card, M. E. (1960), "Investigation of the buckling strength of corrugated webs in shear." NASA Tech. Note D-424, Nat. Aeronautics and Space Admin. (NASA), Washington, D. C.

[7] Hussain, M. I., and Libove, C. (1976), "Trapezoidally Corrugated Plates in Shear." J. Struct. Div., ASCE, 102(ST5), 1109–1131.

[8] Rothwell, A. (1968), "The Shear Stiffness of Flat-sided Corrugated Webs." Aeronaut. Quart., Aug., 1968, 224-234.

[9] Omidvar, B. (1998), "Shear Coefficient in Orthotropic Thin-Walled Composite Beams." J. Composite Construct., ASCE, 2(1), 46–56.

[10] Stephen, N. G. (1997), "Mindlin Plate Theory: Best Shear Coefficient and Higher Spectra Validity." J. Sound Vib., 202(4), 539–553.

(Received September 14,2001)